

Table and Figure Captions

Tables

Table 1 pH, Ash contents, elemental compositions, atomic ratios, and SSA of the CBR and CBR-biochars produced at different pyrolysis temperatures.

Table 2 Parameters of Freundlich and Langmuir models for Cr(VI) removal.

Table 1

pH, ash, elemental composition, atomic ratio, surface area											
Sample	pH	pH _{PZC}	Ash(%)	C (%)	H (%)	N (%)	O (%)	H/C	O/C	(O+N)/C	SSA(m ² /g)
CBR	4.02	3.89	6.12	44.12	5.65	4.24	45.99	1.537	0.782	0.864	0.447
CBR300	6.08	5.85	14.18	56.53	3.86	5.07	42.26	0.819	0.561	0.638	0.986
CBR400	6.89	6.63	20.07	65.68	3.70	5.11	25.51	0.676	0.292	0.358	1.420
CBR500	7.03	6.82	20.11	71.95	3.08	4.69	20.28	0.514	0.211	0.267	7.155
CBR600	8.92	8.74	21.43	73.36	2.78	4.47	19.39	0.455	0.198	0.250	58.232

Table 2

Samples	Freundlich			Langmuir		
	K _F	n	R ²	q _e	b	R ²
CBR	3.89	1.43	0.99	40.99	4.32	0.546
CBR300	2.53	1.43	0.97	37.35	3.35	0.501
CBR400	1.70	1.19	0.99	39.75	4.04	0.504
CBR500	2.34	1.23	0.99	41.43	3.49	0.503
CBR600	4.52	1.45	0.98	42.83	3.58	0.506

Figures

Fig.1. Functional groups present on CBR and CBR-chars inferred from FT-IR (cm^{-1}).

Fig.2. Effects of initial pH on Cr(VI) removal efficiency of CBR and CBR-derived chars at initial Cr(VI) concentration of 50 mg L^{-1} .

Fig.3 Effects of time on Cr concentration at initial pH of 2, and Cr(VI) concentration of 50 mg L^{-1}

Fig.4. Effects of initial Cr(VI) concentration on Cr(VI) removals by CBR and CBR-derived chars at pH 2.

Fig.5. Effects of addition amounts of CBR or CBR-chars on Cr(VI) removal efficiency at initial pH 2 and Cr(VI) concentration 50 mg L^{-1} .

Fig.6. Functional groups present on CBR and CBR-chars inferred from FT-IR (cm^{-1}) after Cr adsorption under the conditions of initial pH of 2, Cr(VI) concentration of 50 mg L^{-1} , and adsorbent dosage of 5 g L^{-1} .

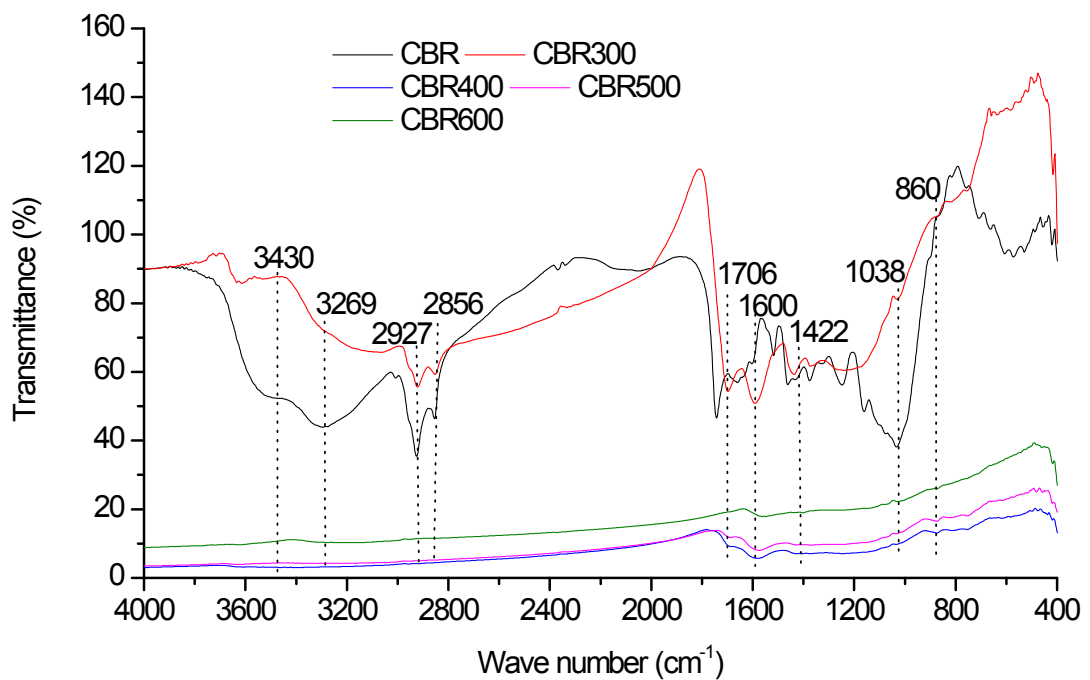


Fig.1

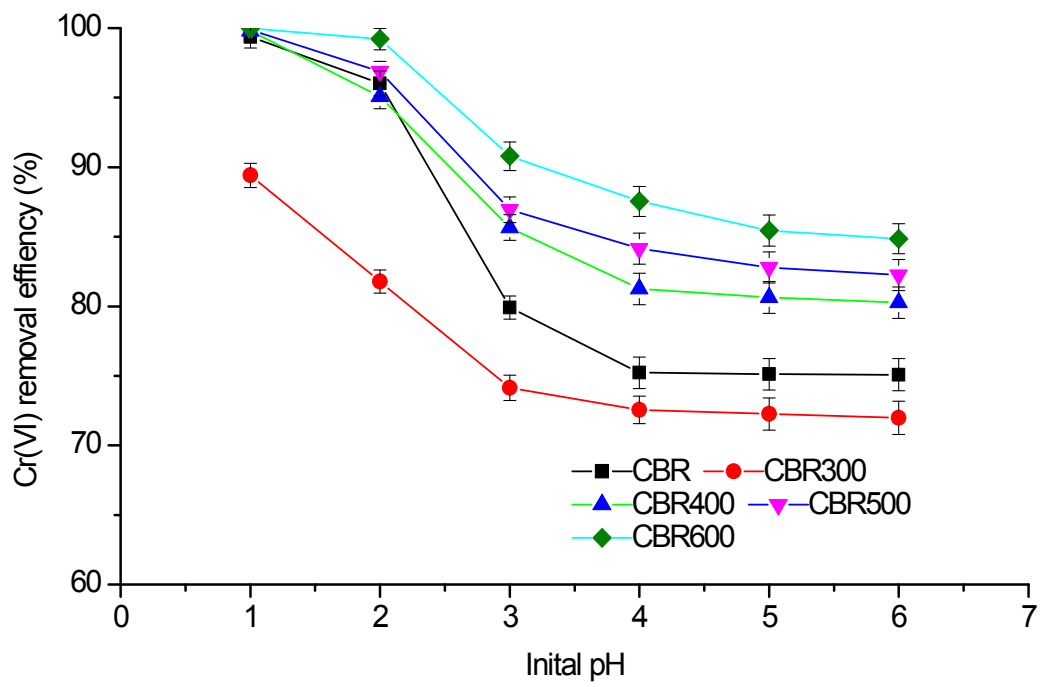


Fig.2

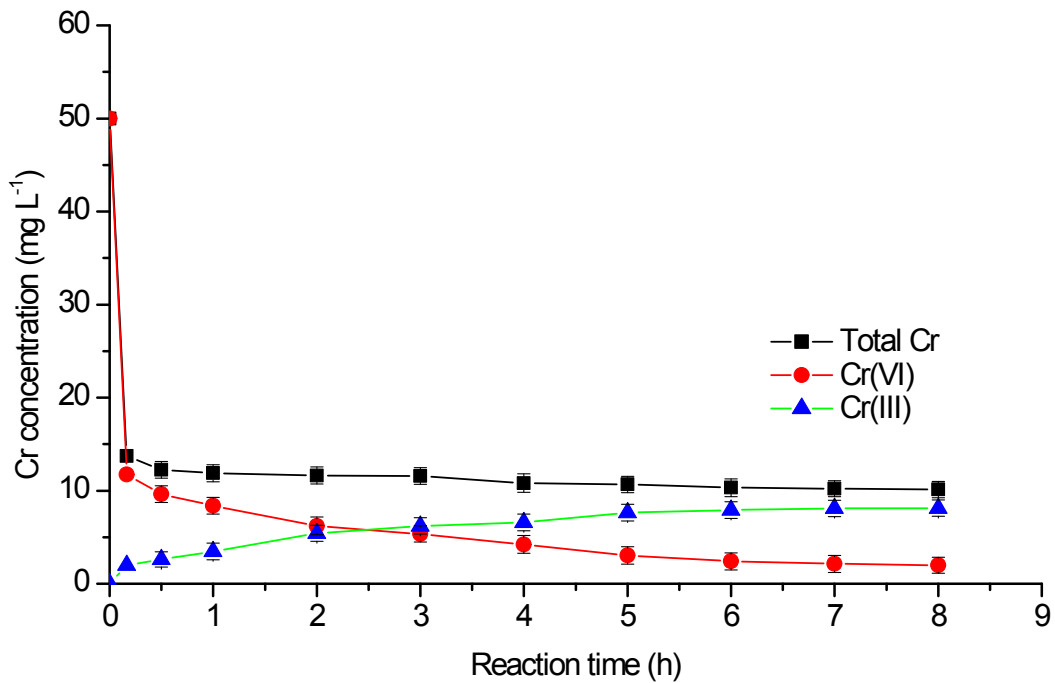


Fig.3

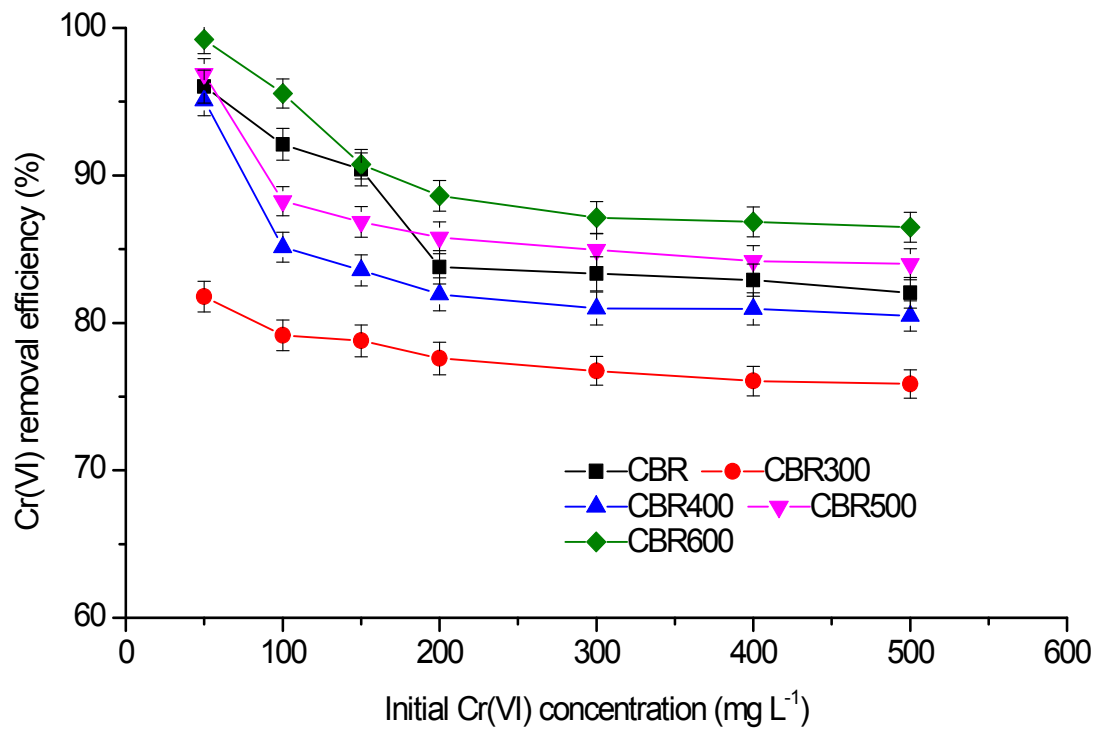


Fig.4

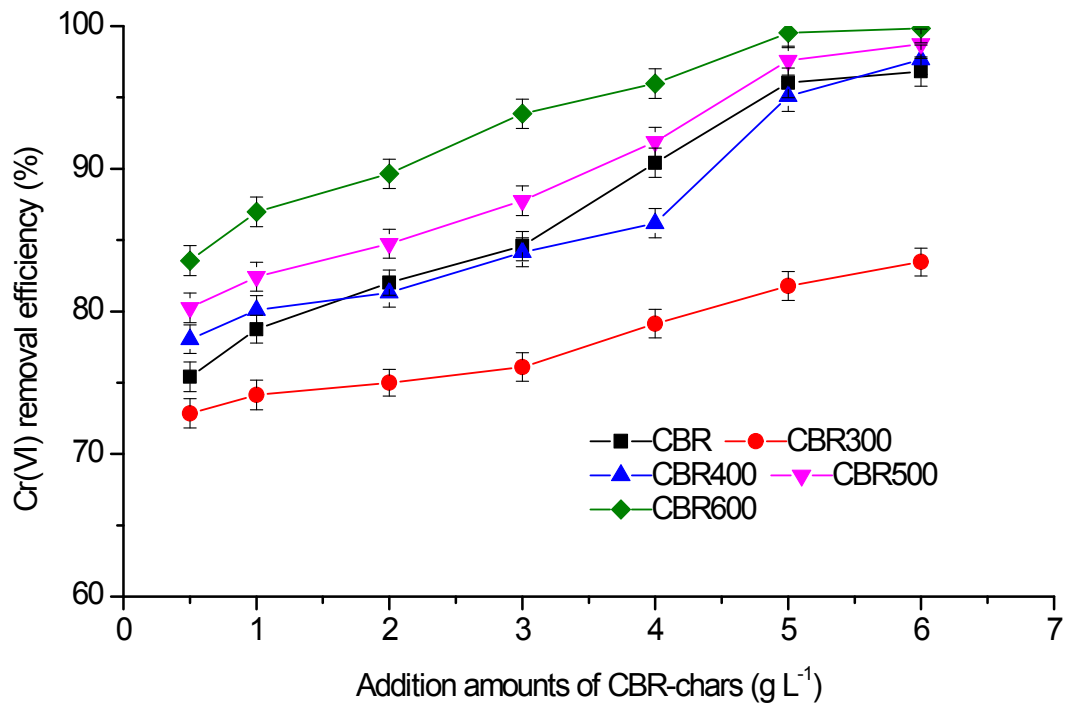


Fig.5

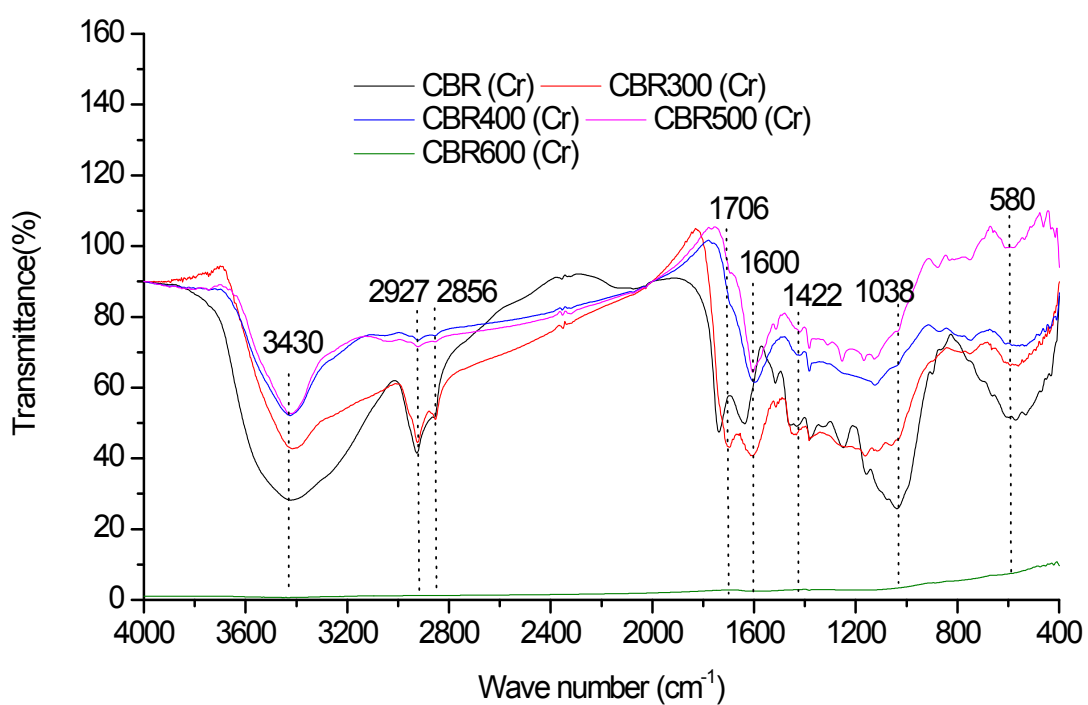


Fig.6